Thin Solid Films 520 (2011) 1608–1611

Contents lists available at SciVerse ScienceDirect

Thin Solid Films

journal homepage: www.elsevier.com/locate/tsf

Paraffin wax passivation layer improvements in electrical characteristics of bottom gate amorphous indium–gallium–zinc oxide thin-film transistors

Geng-Wei Chang [a], Ting-Chang Chang [b,*], Yong-En Syu [b], Tsung-Ming Tsai [c], Kuan-Chang Chang [c], Chun-Hao Tu [d], Fu-Yen Jian [b], Ya-Chi Hung [c], Ya-Hsiang Tai [a]

[a] Department of Photonics & Institute of Electro-Optical Engineering, National Chiao Tung University, Hsin-Chu, 300, Taiwan, ROC
[b] Department of Physics and Center for Nanoscience & Nanotechnology, National Sun Yat-sen University, 70 Lien-hai Road, Kaohsiung, Taiwan, ROC
[c] Institute of Materials Science and Engineering, National Sun Yat-Sen University, Kaohsiung, 70 Lien-hai Road, Kaohsiung, 804, Taiwan, ROC
[d] Institute of Electronics, National Chiao Tung University, Hsin-Chu, 300, Taiwan, ROC

ARTICLE INFO

Available online 6 September 2011

Keywords:
Indium Gallium Zinc Oxide (IGZO)
Thin film transistors (TFTs)
Passivation layer

ABSTRACT

In this research, paraffin wax is employed as the passivation layer of the bottom gate amorphous indium–gallium–zinc oxide thin-film transistors (a-IGZO TFTs), and it is formed by sol–gel process in the atmosphere. The high yield and low cost passivation layer of sol–gel process technology has attracted much attention for current flat-panel-display manufacturing. Comparing with passivation-free a-IGZO TFTs, passivated devices exhibit a superior stability against positive gate bias stress in different ambient gas, demonstrating that paraffin wax shows gas-resisting characteristics for a-IGZO TFTs application. Furthermore, light-induced stretch-out phenomenon for paraffin wax passivated device is suppressed. This superior stability of the passivated device was attributed to the reduced total density of states (DOS) including the interfacial and semiconductor bulk trap densities.

1. Introduction

Recently, there has been a considerable interest in developing transparent flexible electronic devices such as wearable computers and paper displays. ZnO-based transistors have a great potential to be used in emerging electronic devices including the thin film transistor (TFT) backplanes for flexible displays or transparent active matrix organic light-emitting diode (AMOLED) displays because they offer high mobility [1,2], excellent uniformity, and good transparency to visible light [3]. Furthermore, devices fabrication at low temperature is also attractive for transparent flexible displays. However, threshold voltage variation during bias stress limits the application of a-IGZO TFTs. The instability of a-IGZO TFTs resulted from the adsorption/desorption of gas molecules on the back channel layer [4]. It is crucial for oxide-based transistors to exhibit long term bias-stress stability for practical applications. A suitable passivation layer process development is useful for reliability improvement of a-IGZO TFTs. Passivation layers, such as SiO_x, SiN_x, TiO_x, and Al_2O_3 was deposited by using the plasma enhanced chemical vapor deposition (PECVD) or sputtering under a vacuum environment. However, creating vacuum environment takes considerable amount of time, thus causing the low yield. As a result, a variety of approaches to passivation layers will need to be investigated to improve the stability for the TFTs. In this article, we report a method by sol–gel process for paraffin wax passivation layer formation in a-IGZO TFTs. The high yield and low cost passivation layer of sol–gel process technology has attracted much attention for the application of a-IGZO TFTs. The paraffin wax is a mixture of 26- to 30-carbon alkane hydrocarbons. It is chemically inert because alkane is nonpolar and lacking in functional groups [5]. In addition, the electrical stability test was performed in various ambient environments, such as O_2, and H_2O. Particularly, the paraffin wax passivated device exhibits stable electrical characteristics against positive gate bias stress, demonstrating that paraffin wax has a good passivation ability to resist environmental factor damage. Furthermore, the IGZO TFTs with paraffin wax passivation layer have stable transistor performance under visible-light illumination compare with unpassivated TFTs. This superior stability of the passivated device is attributed to the reduced total density of states (DOS) including the interfacial and semiconductor bulk trap densities.

2. Experiment

The bottom gate a-IGZO TFTs using coplanar structure were produced on glass substrate. First, the tri-layer films of Ti/Al/Ti (50/200/50 nm) were deposited and patterned via photolithography on a glass substrate to form the gate electrodes. The sputtering was carried out in ambient Ar gas, at a chamber pressure of 5 mTorr, and with a plasma discharge power of 300 W. Then, a 300 nm SiO_x film was deposited by using PECVD at a substrate temperature of 370 °C as gate insulator. The Ti/Al/Ti (50/200/50 nm) source/drain electrodes were deposited by sputtering and patterned into the dimension of

* Corresponding author.
E-mail address: tcchang@mail.phys.nsysu.edu.tw (T.-C. Chang).

0040-6090/$ – see front matter © 2011 Elsevier B.V. All rights reserved.
doi:10.1016/j.tsf.2011.08.104

channel width/length = 10–15 μm/10 μm. A 30-nm-thick a-IGZO channel layer was formed by dc magnetron sputtering using an alloy target of In:Ga:Zn = 1:1:1 at room temperature. The sputtering was carried out in a gas mixture ratio of O_2/Ar = 6.7%, at a chamber pressure of 5 mTorr, and with a plasma discharge power of 300 W. After defining the active region, the devices were annealed in an oven at 150 °C for 20 min. In addition, thermal-annealed a-IGZO TFTs were passivated by spin-coated paraffin wax film. The electrical properties of a-IGZO TFTs with length = 10 μm and width = 10 μm were analyzed by using Agilent 4156-C system at 30 °C. The linear mobility was extracted by normal method of the square root normalized drain current ($NI_D = I_D \times L/W$) verse gate voltage (V_G) plot and the threshold voltage (V_T) is defined as the V_G of the NI_D reaching 1 nA. The sub-threshold slope (SS) was extracted from NI_D in the sub-threshold region (the NI_D from 10^{-11} A to 10^{-9} A). Also, Fourier transform infrared spectrosocopy (FTIR) was used to determine the bonding type of the passivation layer.

3. Results and discussion

The transfer characteristics (I_D–V_G) for the unpassivated and paraffin wax passivated of a-IGZO TFTs at a fixed V_D = 5 V are shown in Fig. 1. The electrical properties of unpassivated device shows the mobility of 11.73 cm^2/Vs, V_T of 0.87 V, and SS of 0.23 V/decade. For paraffin wax passivated device, it exhibited similar characteristics, such as the mobility of 12.02 cm^2/Vs, and SS of 0.21 V/decade. However, it is noticeab that V_T has a parallel negative shift, from 0.87 V to 0.28 V. a-IGZO TFTs are degraded when oxide channel is exposed to hydrogen during the deposition of the passivation layer [6]. A negative V_T shift is created due to the hydrogen dissociated from the paraffin wax may act as a donor in n-type IGZO. As shown in Fig. 2, the FTIR spectrum of the passivation layer exhibits symmetric and asymmetric C – H stretching vibrations (2930, 2890, and 2853 cm^{-1}), CH_2 (1467 and 723 cm^{-1}), and CH_3 (1379 cm^{-1}) [7–9]. At the 3000–2700 cm^{-1} region for C – H stretching bands, it can be noted that significant differences in the relative intensity of the bands are due to the change of the alkyl chain length. Another two bands which can be used to differentiate the chain length are the bands at 1467 and 1379 cm^{-1}, which represent methylene (CH_2) and methyl (CH_3) group bending vibrational bands, respectively. [10] The materials of paraffin layer are constituted by both carbon and hydrogen from the FTIR analysis. The hydrogen in the paraffin wax layer makes the IGZO layer more conductive. Thus, the threshold voltage of a-IGZO TFTs shifted negatively after coating the paraffin wax passivation layer.

The passivation effects on the device stability were also investigated. The stress condition was set at V_G = 30 V for 1000 seconds. Fig. 3 and 4

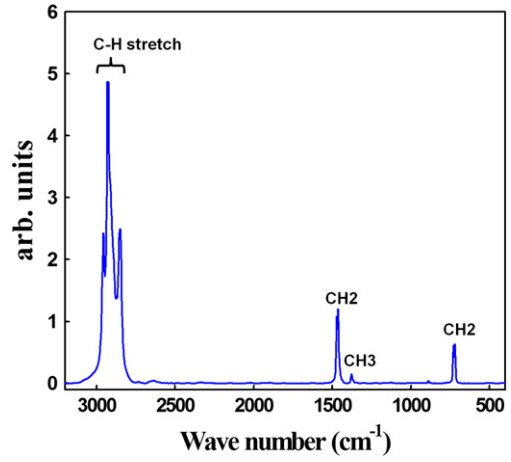

Fig. 2. FTIR spectrum of the paraffin wax exhibits a sharp C – H bonding type at around 2890 cm^{-1}, CH_2 at around 1467 and 723 cm^{-1}, and CH_3 at around 1379 cm^{-1}.

exhibit the characteristics for stressed a-IGZO TFTs without and with passivation layer, respectively. After positive gate bias stress, the electrical transfer characteristics were divided into two branches. The upper part was in the turn-on state, and the lower part was located in deep sub-threshold regime. The positive gate bias stress led to the shift of the upper I_D–V_G curve in the positive direction for both the w/o or w/paraffin wax passivation device. The V_T shift in the oxide-based TFTs was contributed by charge trapping phenomenon [11,12], charge injection [13], and channel defects [14]. The injected electrons during positive gate bias are trapped in the gate dielectric and/or at the channel/gate dielectric interface, resulting in a less effective gate voltage, thus a larger positive gate voltage is required to turn on the drain current. However, an apparent hump effect in the lower transfer curves during positive bias stress for the device without passivation was observed. The hump transfer curve seems to be contributed by a combination of a dominant transistor and a parasitic transistor [15]. The H_2O absorption at backchannel can be formation of H_2O^+ induces the delocalized electron carrier on the back channel, which serves as donors to develop a conductive back channel performed as a parasitic transistor [16,17]. In contrast, the hump was suppressed for the device with paraffin wax passivation. This indicates that paraffin wax layer effectively avoids H_2O absorbing in a-IGZO back channel surface. The electrical stress reliability can be improved by suppressing the hump effect.

The instability of a-IGZO TFTs results from the adsorption/desorption of gas molecules from ambient on back channel layer [4]. In order to

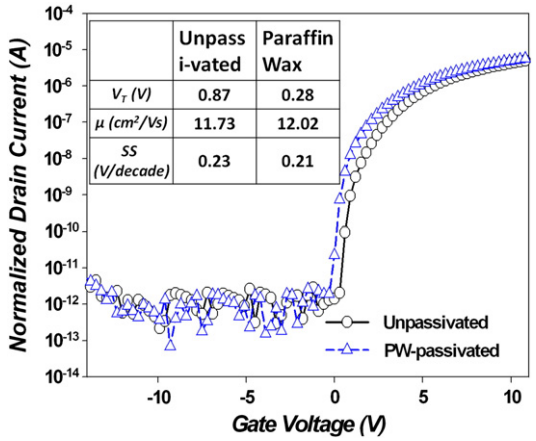

Fig. 1. Transfer characteristics for the as-fabricated a-IGZO TFTs w/o and w/paraffin wax passivation layer.

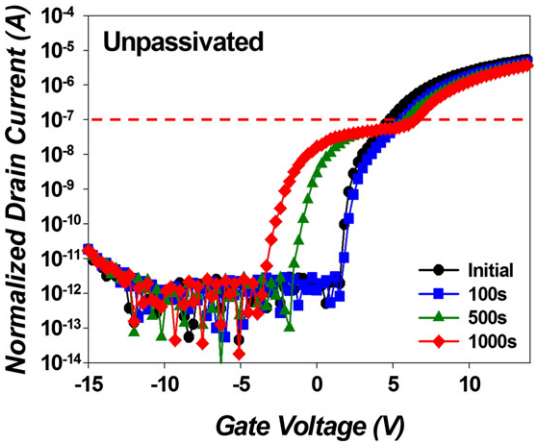

Fig. 3. Transfer characteristics of the a-IGZO TFTs w/o paraffin wax passivation during positive bias stress (PBS) under the atmosphere ambient.

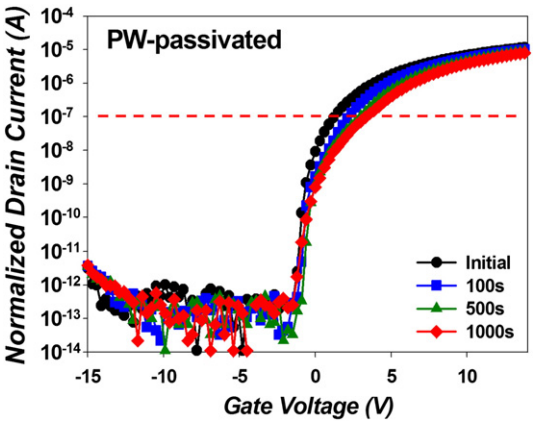

Fig. 4. Transfer characteristics of the a-IGZO TFTs w/paraffin wax passivation during positive bias stress (PBS) under the atmosphere ambient.

confirm the paraffin wax layer can effectively prevent gas molecules in the atmosphere affecting the stability of a-IGZO TFTs under positive gate bias stress, electrical stress test for the device with paraffin wax was performed for atmosphere test including O_2, H_2O vapor (N_2 99% + H_2O), and vacuum (2.5×10^{-3} Torr). Fig. 5(a) shows a higher negative shift more than −4 V occurs after positive gate bias stress for unpassivated device in both air atmosphere and H_2O environments. In contrast, the device with paraffin wax has good electrical stress reliability. Fig. 5(b) shows the corresponding V_T variations of the device with paraffin wax under positive gate bias stress in various environments. The device was stable in O_2 atmosphere, in H_2O vapor, and in vacuum, and had a slight positive threshold shift smaller than 1 V. Therefore,

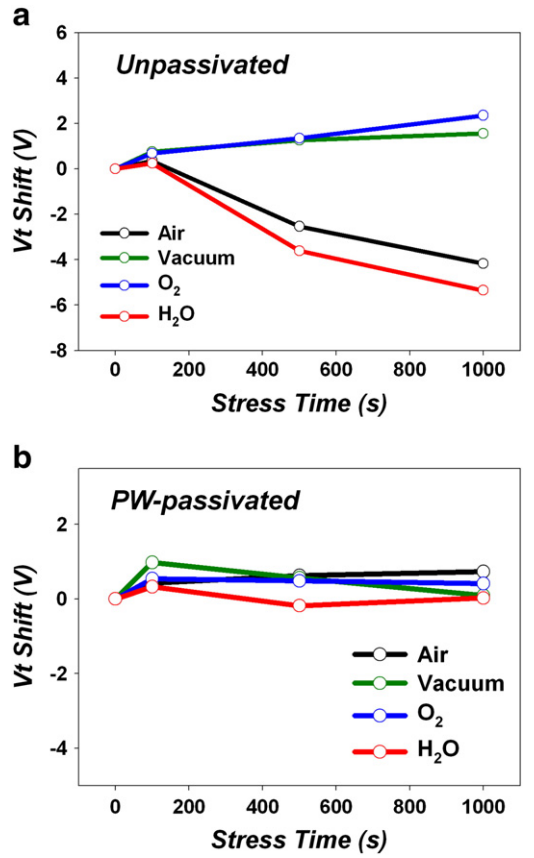

Fig. 5. Dependence between stress time and V_T shift for (a) unpassivated and (b) passivated device during positive gate bias stress under different ambient atmospheres.

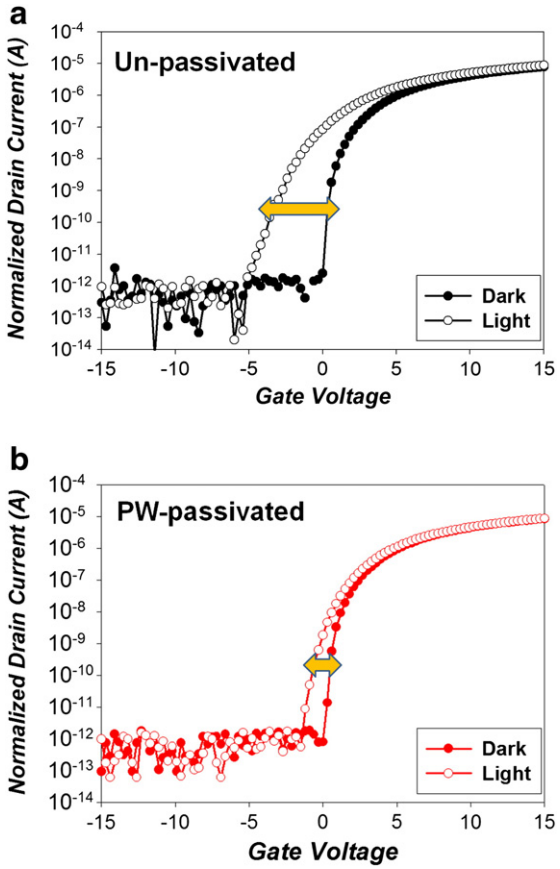

Fig. 6. Transfer I–V characteristics measured in dark and under light illumination for (a) the device w/o and (b) w/paraffin wax passivation layer.

the paraffin wax passivation layer can enhance the bias stress stability of a-IGZO TFTs under different atmospheres.

Fig. 6(a) and (b) shows the transfer I_d–V_g characteristics of the device without and with paraffin wax passivation layer, respectively, in dark and under light illumination with light intensity of 10,000 lx from halogen lamp. The instability of Zn-based TFTs under light illumination was attributed to the light-induced carrier generation

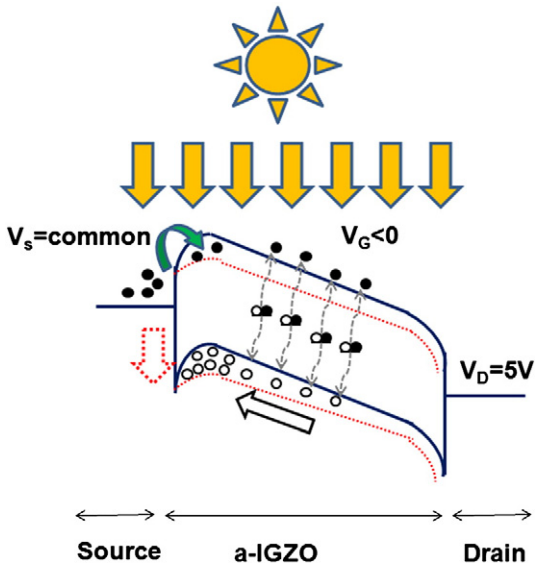

Fig. 7. Schematic energy band diagram under light illumination operated in off-state (V_g<0 V, V_d>0 V).

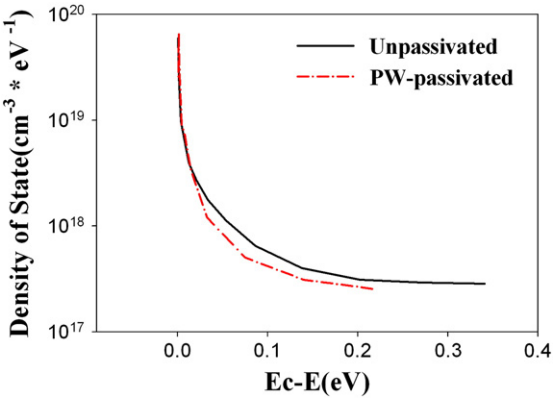

Fig. 8. Calculated DOS distribution as a function of the energy (Ec-E) for the device w/o or w/paraffin wax passivation layer.

[18]. For the unpassivated device, the transfer curve exhibits an apparent stretch-out phenomenon while under light. When under light illumination, electron–hole pairs could be generated from trap-assisted tunneling and the generated holes would drift to the source side and lower the barrier. The source side barrier lowering enhances electrons injection from the source and causes an apparent subthreshold leakage current (as shown in Fig. 7) [19]. However, there is only a small amount of electron–hole pair production under light illumination for the device with paraffin wax coating due to a reduced density of state (DOS) in IGZO bulk. Therefore, the stretch-out phenomenon of transfer curve can be suppressed with paraffin wax passivation.

Fig. 8 shows the DOS distribution as a function of the energy for the device without and with paraffin wax. The DOS extracted reported in the previous work [20]. The total DOS for passivation device was much smaller than that of unpassivation device over the entire tailing energy range extracted. This further suggests that paraffin wax layer devices have superior performance. The total DOS value at a specific energy is the summation of the interfacial trap density (Nit) and the semiconductor film (Nss) because both trap states hinder rise of the E_F level at the interface with increasing V_{GS} ($>V_{FB}$). Considering that the IGZO channel layers for both devices were formed under identical deposition conditions, the difference in the total distribution can explained by the presence of the passivation layer. This suggests that the Nss for passivation-free device is larger than that of the passivated device. Therefore, the better light stability for passivated device can be attributed to the reduced Nss at the IGZO bulk film.

4. Conclusion

In conclusion, the sol–gel-processed paraffin wax passivation layer for the a-IGZO TFTs was discussed in this study. The device after paraffin wax passivation process shows a negative V_T shift that result from the hydrogen may act as a donor in n-type IGZO, making the TFTs more conductive. From the measurements in different gas environment, the passivated device exhibits a superior stability against positive gate bias stress, demonstrating that paraffin wax has a good passivation ability to prevent gas absorption. In addition, the light-induced stretch-out phenomenon was suppressed for a-IGZO TFTs with paraffin wax passivation layer. Furthermore, the paraffin wax passivation layer formation is low cost and high throughput for current flat-panel-display manufacturing.

Acknowledgment

This work was performed at the National Science Council Core Facilities Laboratory for Nano-Science and Nano-Technology in Kaohsiung-Pingtung area and was supported by the National Science Council of the Republic of China under Contract Nos. NSC100-2120-M-110-003, NSC97-2112-M-110-009-MY3 and NSC99-2221-E-009-121.

Reference

[1] H. Yabuta, M. Sano, K. Abe, T. Aiba, T. Den, K. Nomura, T. Kamiya, H. Hosono, Appl. Phys. Lett. 89 (2006) 112123.
[2] Y.H. Yang, S.S. Yang, K.S. Chou, IEEE Electron Device Lett. 31 (9) (2010) 969.
[3] T.C. Chen, T.C. Chang, C.T. Tsai1, T.Y. Hsieh, S.C. Chen, C.S. Lin, M.C. Hung, C.H. Tu, J.J. Chang, P.L. Chen, Appl. Phys. Lett. 97 (2010) 112104.
[4] S.Y. Sung, J.H. Choi, U.B. Han, K.C. Lee, J.H. Lee, J.H. Lee, J.J. Kim, W. Lim, S.J. Pearton, D.P. Norton, Y.W. Heo, Appl. Phys. Lett. 96 (2010) 102107.
[5] D. Choi, D. Wang, I.T. Bae, J. Xiao, Z. Nie, W. Wang, V.V. Viswanathan, Y.J. Lee, J.G. Zhang, G.L. Graff, Z. Yang, J. Liu, Nano Lett. 10 (2010) 2799.
[6] M. Kim, J.H. Jeong, H.J. Lee, T.K. Ahn, H.S. Shin, J.S. Park, J.K. Jeong, Y.G. Mo, H.D. Kim, Appl. Phys. Lett. 90 (2007) 212114.
[7] R.A. MacPhail, H.L. Strauss, R.G. Snyder, C.A. Elliger, J. Phys. Chem. 88 (1984) 334.
[8] D. Biily Yang, Wakamatsu Tomoyo, Surf. Interface Anal. 24 (1996) 803.
[9] D. Atek, N. Belhaneche-Bensemra, Eur. Polym. J. 41 (2005) 707.
[10] J.F. Rabolt, F.C. Burns, N.E. Schlotter, J.D. Swalen, J. Phys. Chem. 78 (1984) 946.
[11] R.B.M. Cross, M.M. De Souza, Appl. Lett. 89 (2006) 263513.
[12] Y. Vygranenko, K. Wang, A. Nathan, Appl. Phys. Lett. 91 (2007) 263508.
[13] A. Suresh, J.F. Muth, Appl. Phys. Lett. 92 (2008) 033502.
[14] K. Nomura, T. Kamiya, M. Hirano, H. Hosono, Appl. Phys. Lett. 95 (2009) 013502.
[15] C.F. Huang, C.Y. Peng, Y.J. Yang, H.C. Sun, H.C. Chang, P.S. Kuo, H.L. Chang, C.Z. Liu, C.W. Liu, IEEE Electron Device Lett. 29 (2008) 1332.
[16] J.S. Park, J.K. Jeong, H.J. Chung, Y.G. Mo, H.D. Kim, Appl. Phys. Lett. 92 (2008) 072104.
[17] N. Yamazoe, J. Fuchigami, M. Kishikawa, T. Seiyama, Surf. Sci. 96 (1979) 335.
[18] P. Görrn, M. Lehnhardt, T. Riedl, W. Kowalsky, Appl. Phys. Lett. 91 (2007) 193504.
[19] Y. Kamada, S. Fujita, T. Hiramatsu, T. Matsuda, M. Furuta, T. Hirao, Solid-State Electron. 54 (2010) 1392.
[20] M. Kimura, T. Nakanishi, K. Nomura, T. Kamiya, H. Hosono, Appl. Phys. Lett. 92 (2008) 133512.